

# Communication

## Tension-Tension-Fatigue Behaviors of a Zr-Based Bulk-Metallic-Glass-Matrix Composite

J.W. QIAO, S.G. MA, G.Y. WANG, F. JIANG, P.K. LIAW, and Y. ZHANG

An improved tension-fatigue limit of 473 MPa is gained for  $Zr_{58.5}Ti_{14.3}Nb_{5.2}Cu_{6.1}Ni_{4.9}Be_{11.0}$  bulk-metallic-glass-matrix composites (BMGMCs). High volume-fraction dendrites within the glass matrix induce increased effectiveness on the blunting and propagating resistance of the fatigue-crack tip. Each fine striation is created during one stress cycle on the basis of analysis of experiments and calculations. A distinguishingly decreased crack-growth rate for the BMGMCs, compared to the monolithic BMGs, prevails, due to the plastic deformation of the dendrites, evidenced by the synchrotron X-ray results.

DOI: 10.1007/s11661-011-0788-7

© The Minerals, Metals & Materials Society and ASM International 2011

Bulk-metallic glasses (BMGs) exhibit superior properties at ambient temperature, such as high strengths, large elastic limits, and excellent corrosion and wear resistance, which renders them potential candidates as structural engineering materials.<sup>[1]</sup> However, the localized shear banding upon loading induces the catastrophic failure, restricting the practical engineering applications. Recently, newly developed *in-situ* bulk-metallic-glass-matrix composites (BMGMCs), including the ductile dendrites within the glass matrix, demonstrate significantly improved toughness, especially with the tensile ductility, by tuning the compositions<sup>[2,3]</sup> or tailoring the microstructures.<sup>[4,5]</sup> Microscopically, the plastic-deformation mechanism of *in-situ* BMGMCs is characterized by the multiplication of shear bands, caused by the impediment of crystalline phases to the operation of shear bands.<sup>[2-4]</sup> The possible micromechanism of the plastic deformation could be the severe lattice distortion and local amorphization in the dendrites, as well as pileups of dislocations close to the interface between the dendrites and the glass matrix.<sup>[6]</sup>

J.W. QIAO, Researcher, is with the College of Materials Science and Engineering, Taiyuan University of Technology, Taiyuan 030024, P.R. China. Contact e-mail: qiaojunwei@gmail.com S.G. MA, Doctoral Student, and Y. ZHANG, Professor, are with the State Key Laboratory for Advanced Metals and Materials, University of Science and Technology Beijing, Beijing 100083, P.R. China. G.Y. WANG and F. JIANG, Researchers, and P.K. LIAW, Professor, are with the Department of Materials Science and Engineering, University of Tennessee, Knoxville, TN 37996-2200.

Manuscript submitted December 28, 2010.

Article published online July 6, 2011

As a result, an improved plasticity is available for BMGMCs.

The fatigue behavior is a very important characteristic for applications of structural materials. Components are frequently bearing cyclic loads, with the load being time dependent, but repetitive, and almost 90 pct of the service failure is caused by the fatigue fracture.<sup>[7]</sup> However, very limited studies<sup>[8-11]</sup> are focused on the fatigue behaviors of BMGMCs. In this study, the high-cycle fatigue behaviors of a Zr-based BMGMC with the composition of  $Zr_{58.5}Ti_{14.3}Nb_{5.2}Cu_{6.1}Ni_{4.9}Be_{11.0}$  in atomic percent are characterized by the tension-tension fatigue, and the relevant fatigue-deformation mechanism is explored.

The  $Zr_{58.5}Ti_{14.3}Nb_{5.2}Cu_{6.1}Ni_{4.9}Be_{11.0}$  BMGMC was prepared in a cylinder shape with a diameter of ~5 mm, fabricated by the copper-mold-suction casting. The detailed procedures of the fabrication can be found in Reference 6. The cross section of the as-cast sample was investigated using scanning electron microscopy (SEM). The rod-shaped cast samples were machined into buttonhead fatigue specimens with a notch. The geometry of the notched samples and the setup for the tension-tension fatigue can be found elsewhere.<sup>[12]</sup> The stress-concentration factor is 1.5 at the notched section.<sup>[13]</sup> Samples were tested at various stress ranges and at room temperature 296 K (23 °C) with an *R* ratio ( $R = \sigma_{\min}/\sigma_{\max}$ , where  $\sigma_{\min}$  and  $\sigma_{\max}$  are the applied minimum and maximum stresses, respectively) of 0.1 under a load-control mode, using a sinusoidal waveform at a frequency of 10 Hz. The fatigue-failure samples were examined by SEM. The synchrotron X-ray experiments were carried out at the Argonne National Laboratory (ANL, Argonne, IL). The monochromatic synchrotron high-energy X-ray beam with an energy of 115 KeV penetrated the specimens, and the transmission-diffraction patterns were collected by a two-dimensional (2-D) detector.

Figure 1(a) shows the microstructures of the  $Zr_{58.5}Ti_{14.3}Nb_{5.2}Cu_{6.1}Ni_{4.9}Be_{11.0}$  BMGMC. It can be seen that the dendrites (white contrast) are uniformly distributed within the featureless glass matrix. The composition of the dendrites is rich in the elements of Zr, Ti, and Ni.<sup>[6]</sup> The spacing of the dendritic arms is about 2 to 4  $\mu\text{m}$ , and the volume fraction is approximately 58 pct. We take advantage of the synchrotron high-energy X-ray, which penetrates the bulk specimen to obtain the bulk rather than surface structural information. The high-energy X-ray profile, shown in Figure 1(b), indicates that the peaks (labeled with *(hkl)* values) for the body-centered-cubic (bcc)  $\beta$ (beta)-Zr solid solution are superimposed on the broad diffuse-scattering amorphous maxima, further identifying the dual-phase structure.

Figure 2 shows the stress-life behavior of the present composites (the profiles of the specimens tested in the inset) and the reported composites,<sup>[8,9]</sup> which have similar dual-phase structures, including the same elemental Zr, Ti, Cu, Ni, Be, and Nb. It was demonstrated that different alloy compositions, composed of different elements, obviously lead to the different fatigue properties.<sup>[14]</sup> Thus, the fatigue behaviors of the same alloy system BMGMCs are compared, as shown in Figure 2.

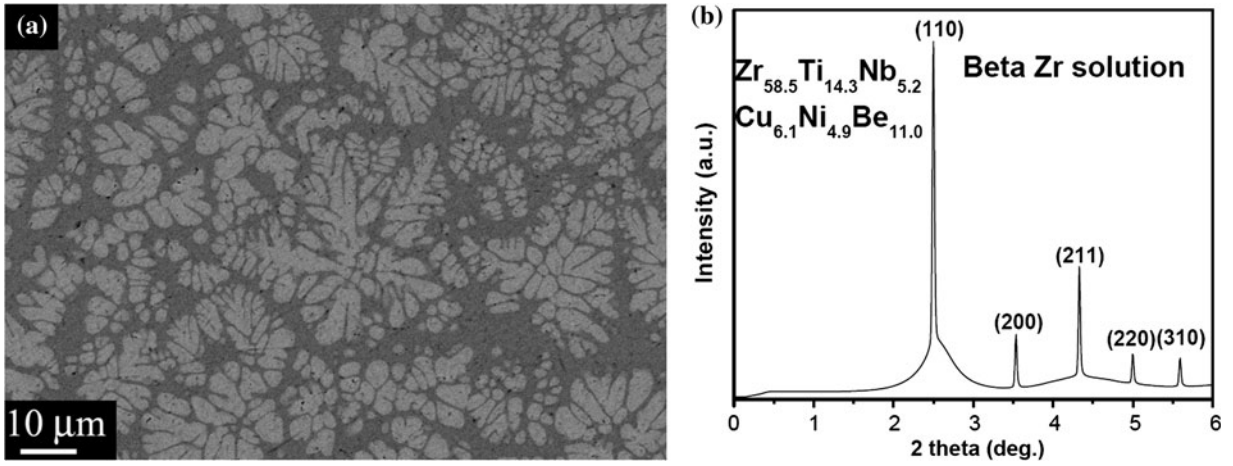


Fig. 1—(a) Microstructure and the (b) high-energy X-ray profile of the  $Zr_{58.5}Ti_{14.3}Nb_{5.2}Cu_{6.1}Ni_{4.9}Be_{11.0}$  BMGMC.

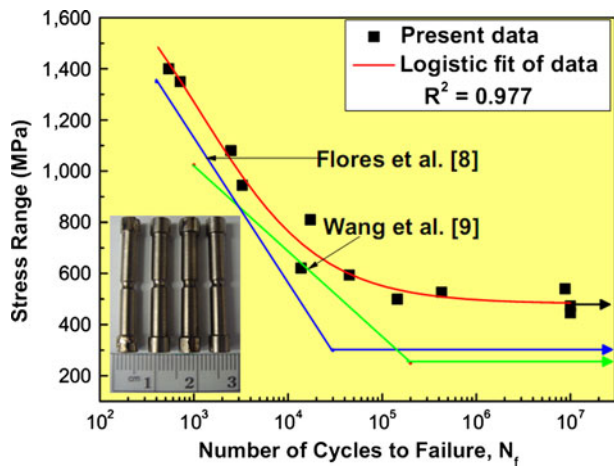


Fig. 2—Stress-life behavior of the present composites and the reported composites; the profiles of the specimens tested in the inset.

It should be noted that the stress range  $\Delta\sigma = \sigma_{\max} - \sigma_{\min}$ . The present composites exhibit super fatigue properties. The fatigue-endurance limit,  $\sigma_L$ , based on  $\Delta\sigma$ , is 473 MPa. For comparison, Flores *et al.*<sup>[8]</sup> reported a  $\sigma_L$  upon the four-point bending (rectangle specimen with width of 38.1 mm and thickness of 2.1 to 2.9 mm) fatigue with a value of 300 MPa, and Wang *et al.*<sup>[9]</sup> obtained a  $\sigma_L$  upon the tension-tension (buttonhead fatigue specimen with a taper notch) fatigue of 239 MPa for the same composites. Additionally, it is noted that all the present data are above the reported data, demonstrating a longer lifetime for the present composites when the composites are subjected to the same stress ranges. For actual engineering applications, the  $\Delta\sigma$  and  $N_f$  is well fitted using a logistic equation:

$$\Delta\sigma = A_2 + \frac{A_1 - A_2}{1 + \left(\frac{\lg N_f}{X_0}\right)^p} \quad [1]$$

where  $A_1$ ,  $A_2$ , and  $X_0$  are constants with the values of  $1985.91 \pm 570.70$  MPa,  $481.73 \pm 6.82$  MPa, and

$1154.31 \pm 1391.37$ , respectively, and the exponent,  $p$ , is  $0.68 \pm 0.22$ . The great fitting ( $R^2 = 0.977$ ) reveals a high reliability of the present composites.

For a specimen upon loading, the components of the stresses include the normal ( $\sigma$ ) and shear ( $\tau$ ) stresses. The soft coefficient,  $\alpha$ , is employed to characterize the stress state:  $\alpha = \tau_{\max} / \sigma_{\max}$ , where  $\tau_{\max}$  and  $\sigma_{\max}$  are the maximum shear and normal stresses, respectively. The larger the  $\alpha$ , the easier to shear deform for the materials, *i.e.*, the “softer” the materials. For instance, upon uniaxial compression,  $\alpha \approx 2$ , while upon uniaxial tension,  $\alpha \approx 0.5$ . Obviously, mode I dominates upon tensile loading and a crack easily initiates and propagates. That is why a lower tensile fatigue-endurance limit is obtained, compared to that upon bending or compression fatigues when the testing conditions such as  $R$  are the same.<sup>[14]</sup> The present tensile-tension-fatigue data are most conservative for applications.

The stress amplitude,  $\sigma_a = 1/2 (\sigma_{\max} - \sigma_{\min})$ , is normalized by the ultimate tensile strength,  $\sigma_u \sim 1480$  MPa.<sup>[15]</sup> The present composites exhibit an endurance limit at  $\sigma_a / \sigma_u \sim 0.16$ , obviously higher than that regardless of bending ( $\sigma_a / \sigma_u \sim 0.10$ ) or tension ( $\sigma_a / \sigma_u \sim 0.08$ ) for the reported composites.<sup>[8,9]</sup> Above the endurance limit, defined as stresses resulting in lifetime  $>10^7$  cycles, the number of cycles to failure,  $N_f$ , decreases rapidly as  $\sigma_a / \sigma_u$  increases. The crack propagation during the tension-tension fatigue is under mode I, as shown in the inset of Figure 3(a). Only if the final fracture is available does mode II prevail. Because of the stress concentration, a plastic zone forms in the vicinity of the crack tip, causing a crack tip opening and, similarly, crack propagation. It was demonstrated that the ductile dendrites within the glass matrix can effectively blunt the crack tip and hinder its propagation, and the slip along the shear bands can be arrested.<sup>[10]</sup> In addition, the plastic deformation of dendrites can lead to work hardening,<sup>[6]</sup> further stabilizing the crack growth during fatigue. The availability of ductile dendrites near the crack tip can change the crack path due to the localized plastic deformation, reducing the effective stress intensity range.

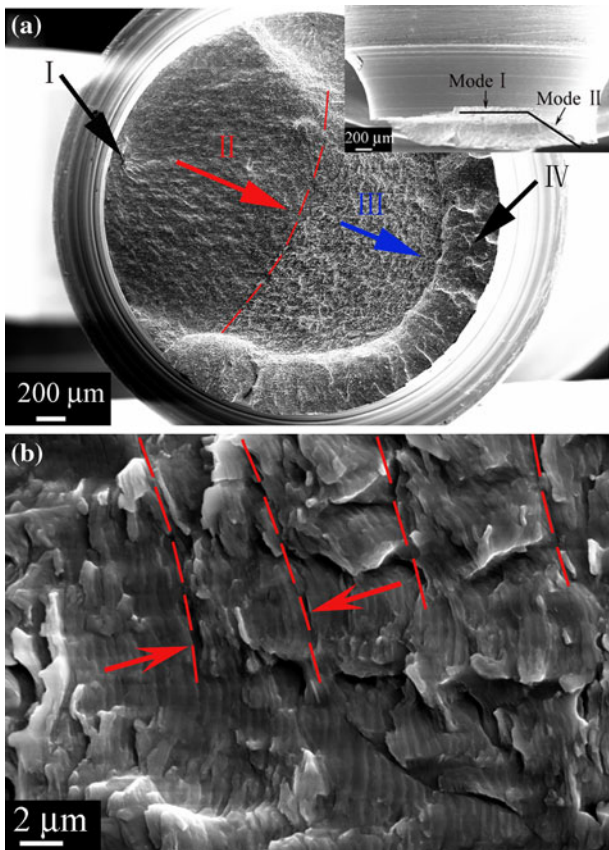


Fig. 3—(a) Overall fatigue fractography of the composites subjected to a stress range of 810 MPa. (b) The enlarged part in stage II, indicated in (a), near the arresting line. The crack propagation during the tension-tension fatigue exhibited in the inset of (a).

For the present composites, the ductile dendrites with a large volume fraction (~58 pct), more than double that (~25 pct) for the reported composites,<sup>[8,9]</sup> constitute a network structure, as presented in Figure 1(a), which more favorably enables the interception between the cracks and the dendrites. The obviously coarsened dendrites, compared to the reported composites,<sup>[8,9]</sup> may result in increased crack tip blunting. Besides, the small spacing between the dendrites has a beneficial effect on the toughness, which gives an increased crack resistance.<sup>[5,16]</sup> For BMGMCs, the crack tip closure or crack tip shielding results from the plastic deformation of the dendrites, and the glass matrix cannot plastically deform. So the blunting of the high-volume fractioned dendrites induces an improved fatigue property.

For further exploration of the improved fatigue-endurance limit, the crack-propagation behavior is investigated. Figure 3(a) shows the overall fatigue fractography of the composites subjected to a stress range of 810 MPa. Four typical fatigue stages,<sup>[12]</sup> (I) the crack-initiation site, (II) the crack-growth region, (III) the fast fracture region, and (IV) the final fracture region, indicated by the arrows, prevail. The initiation site is located in the interior not the surface scratch. A thumbnail shape dominates stage II, and stages II and III can be discerned by an arresting line (dashed line).

Figure 3(b) exhibits an enlarged part in stage II near the arresting line. The crack growth is along the arrow, and the coarse striations (labeled by the dashed line) have a spacing of 4 to 6 μm. Usually, there is a plastic zone ahead of the crack extension. When the crack extends into the glass matrix, the plastic strain is accommodated by the operation of shear bands. The crack easily extends along the shear bands, and the coarsened striations form. Close inspections between the coarse striations reveal dense fine striations, which can be observed between the coarse striations and have a spacing of 330 to 500 nm. Wang *et al.*<sup>[17]</sup> demonstrated that each fine striation corresponds to one stress cycle for monolithic BMGs.

Usually, the crack-growth rate ( $da/dN$ ) in a steady state follows the Paris law:<sup>[18]</sup>

$$\frac{da}{dN} = C(\Delta K)^m \quad [2]$$

where  $C$  is a material constant,  $m$  is the crack-growth exponent with a value of 2 to 4 for ductile metals,<sup>[10]</sup> and  $\Delta K$  is the cycle-stress-intensity factor. Nisitani and Chen<sup>[19]</sup> estimated  $\Delta K$  from the morphology of the fracture surface, using the following equation:

$$\Delta K = \Delta\sigma\sqrt{\pi a}F(\lambda) \quad [3]$$

where  $a$  is the depth of the fatigue-crack tip, and can be found in References 17 and 19, and  $F(\lambda)$  is the boundary-correction factor and defined as follows:

$$F(\lambda) = 0.66 - 0.02398\lambda + 1.664\lambda^2 \quad [4]$$

Here,  $\lambda = a/D$ , where  $D$  is the specimen diameter. In the present study,  $\Delta K$  is calculated to be 30.77 MPa m<sup>1/2</sup>, based on  $\lambda = 0.4$ ,  $C = 1.5 \times 10^{-11}$  MPa m<sup>1/2</sup>,<sup>[10]</sup> and  $m = 3$ ; as a result,  $da/dN = 437$  nm/cycle. The calculation at the final portion of stage II is very close to the experimental data of fine-striation spacings of 330 to 500 nm. It is reasonable to deduce that each fine striation is created during one stress cycle for the present BMGMCs on the basis of the analysis of experiments and calculations. It is noted that the experimental data for the crack-growth rate for the present composites is distinguishingly lower than 720 nm/cycle at the corresponding final portion of stage II for the monolithic BMGs.<sup>[20]</sup> The decreasing crack-growth rate indicates the effective blunting of the ductile dendrites at the crack tip and the increased toughness of the composites. As a consequence, the improved tension-fatigue limit is realized.

The noticeable plastic deformation of the ductile dendrites can be indirectly detected by the synchrotron X-ray. Figures 4(a) and (b) display the diffraction patterns of the sample before and after the fatigue failure at  $\Delta\sigma = 810$  MPa, as indicated in Figure 2, respectively. Due to the ensembled diffraction-intensity distributions of (110) and (211) from the dendrites and the glass matrix, it is not easy to detect the change of the patterns. Here, we choose the diffraction peak (200) as the contrast. After deformation, the continuous diffraction ring dominates instead of the discrete diffraction

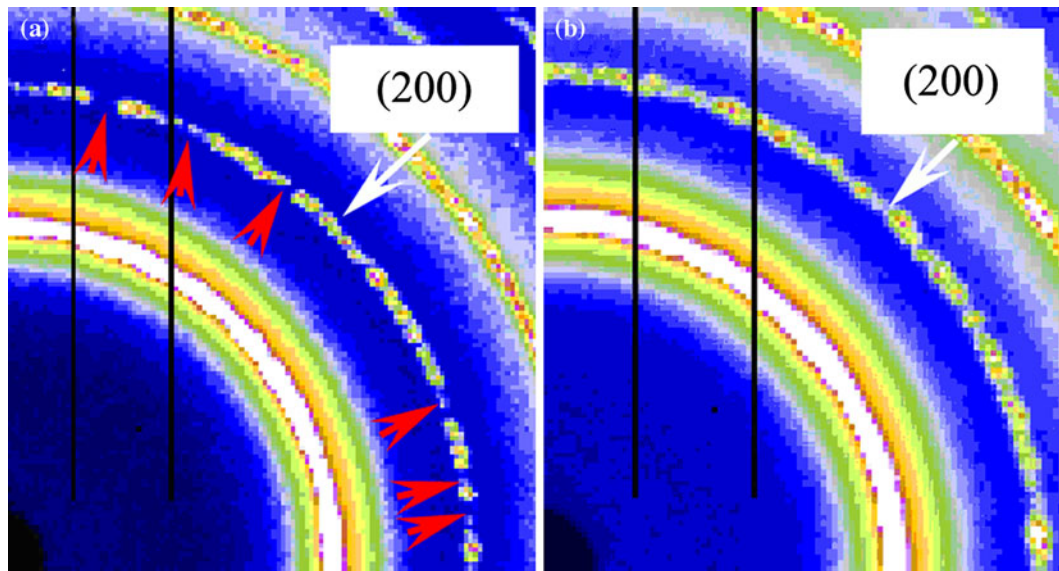


Fig. 4—Diffraction patterns of the sample (a) before and (b) after the fatigue failure at  $\Delta\sigma = 810$  MPa.

spots. During plastic deformation, especially at high stresses, the dendrites can be intercepted by the shear bands,<sup>[5]</sup> together with the formation of intrusions and extrusions at the phase boundary,<sup>[6]</sup> both of which induce decreased grain sizes of dendrites. Thus, a continuous diffraction ring is available. The present analysis gives new evidence of the deformation of dendrites during fatigue.

In conclusion, an improved tension-tension-fatigue limit of 473 MPa, compared to the reported data, is obtained for  $Zr_{58.5}Ti_{14.3}Nb_{5.2}Cu_{6.1}Ni_{4.9}Be_{11.0}$  BMGMCs. The ductile dendrites with a high volume fraction within the glass matrix can effectively blunt the crack tip and hinder its propagation, and the slip along the shear bands can be arrested. Close inspections of the fatigue striations indicate that the spacing of the fine striations from the experimental observation is in accordance to the amount the crack front moved forward during one stress cycle, based on the calculations of the crack-growth rate. The decreased crack-growth rate is available for the present composites, compared to the monolithic BMGs, due to the plastic deformation of ductile dendrites, evidenced by the synchrotron X-ray results. Consequently, the improved tension-fatigue limit prevails.

---

One of the authors (JWQ) acknowledges the financial support of the Program for Talent Introduction, Taiyuan University of Technology (Grant No. tyut-rc201105a). YZ acknowledges the support by the National Basic Research Program of China (the 973 Program) under Contract No. 2007CB613903. PKL is very grateful for the support by the National Science

Foundation Programs (Grant Nos. DMR-0231320, DMR-0421219, DMR-0909037, and CMMI-0900271), with Drs. C.V. Cooper, A. Ardell, D. Finotello, C. Huber, and C. Bouldin as program directors.

## REFERENCES

1. M.K. Miller and P.K. Liaw: *Bulk Metallic Glasses*, Springer, New York, NY, 2007, pp. 18–20.
2. D.C. Hofmann, J.Y. Suh, A. Wiest, G. Duan, M.L. Lind, M.D. Demetriou, and W.L. Johnson: *Nature*, 2008, vol. 451, pp. 1085–90.
3. J.W. Qiao, A.C. Sun, E.W. Huang, Y. Zhang, P.K. Liaw, and C.P. Chuang: *Acta Mater.*, 2011, vol. 59, pp. 4126–37.
4. J.W. Qiao, Y. Zhang, and P.K. Liaw: *Adv. Eng. Mater.*, 2008, vol. 10, pp. 1039–42.
5. J.W. Qiao, S. Wang, Y. Zhang, P.K. Liaw, and G.L. Chen: *Appl. Phys. Lett.*, 2009, vol. 94, p. 151905.
6. J.W. Qiao, Y. Zhang, P.K. Liaw, and G.L. Chen: *Scripta Mater.*, 2009, vol. 61, pp. 1087–90.
7. J.Y. Mann: *Fatigue Materials*, Melbourne University Press, Melbourne, 1967, pp. 1–5.
8. M. Flores, W.L. Johnson, and R.H. Dauskardt: *Scripta Mater.*, 2003, vol. 49, pp. 1181–87.
9. G.Y. Wang, P.K. Liaw, A. Peker, M. Freels, W.H. Peter, R.A. Buchanan, and C.R. Brooks: *Intermetallics*, 2006, vol. 14, pp. 1091–97.
10. K. Boopathy, D.C. Hofmann, W.L. Johnson, and U. Ramamurty: *J. Mater. Res.*, 2009, vol. 24, pp. 3611–19.
11. M.E. Launey, D.C. Hofmann, W.L. Johnson, and R.O. Ritchie: *Proc. Nat. Acad. Sci. USA*, 2009, vol. 106, pp. 4986–91.
12. G.Y. Wang, P.K. Liaw, W.H. Peter, B. Yang, Y. Yokoyama, M.L. Benson, B.A. Green, M.J. Kirkham, S.A. White, T.A. Saleh, R.L. McDaniels, R.V. Steward, R.A. Buchanan, C.T. Liu, and C.R. Brooks: *Intermetallics*, 2004, vol. 12, pp. 885–92.
13. G.Y. Wang, P.K. Liaw, A. Smyth, M. Denda, A. Peker, M. Freels, R.A. Buchanan, and C.R. Brooks: *Rev. Adv. Mater. Sci.*, 2008, vol. 18, pp. 18–22.
14. G.Y. Wang, P.K. Liaw, and M.L. Morrison: *Intermetallics*, 2009, vol. 17, pp. 579–90.
15. J.W. Qiao, Y. Zhang, P. Feng, Q.M. Zhang, and G.L. Chen: *Mater. Sci. Eng. A*, 2009, vol. 515, pp. 141–45.

16. M.E. Launey, D.C. Hofmann, J.-Y. Suh, H. Kozachkov, W.L. Johnson, and R.O. Ritchie: *Appl. Phys. Lett.*, 2009, vol. 94, p. 241910.
17. G.Y. Wang, P.K. Liaw, Y. Yokoyama, A. Inoue, and C.T. Liu: *Mater. Sci. Eng. A*, 2008, vol. 494, pp. 314–23.
18. P.C. Paris and F. Erdogan: *J. Basic Eng.*, 1963, vol. 85, pp. 528–34.
19. H. Nisitani and D.H. Chen: *Trans. Jpn. Soc. Mech. Eng.*, 1984, vol. 50, pp. 1077–82.
20. G.Y. Wang, P.K. Liaw, X.Q. Jin, Y. Yokoyama, E.W. Huang, F. Jiang, L.M. Keer, and A. Inoue: unpublished research, 2011.